

Electric-field-induced widely tunable direct and indirect band gaps in hBN/MoS₂ van der Waals heterostructures

Quan Li,^{‡a} Liang Xu,^{‡*ab} Kai-Wu Luo,^a Xiao-Fei Li,^c Wei-Qing Huang,^a Ling-Ling Wang^a and Ya-Bin Yu^a

^a Department of Applied Physics, School of Physics and Electronics, Hunan University, Changsha 410082, China

^b School of Energy and Mechanical Engineering, Jiangxi University of Science and Technology, Nanchang 330013, China

^c School of Optoelectronic Information, University of Electronic Science and Technology of China, Chengdu 610054, China

* Corresponding author. *E-mail address:* liangxu@hnu.edu.cn

[‡] These authors contributed equally to the work.

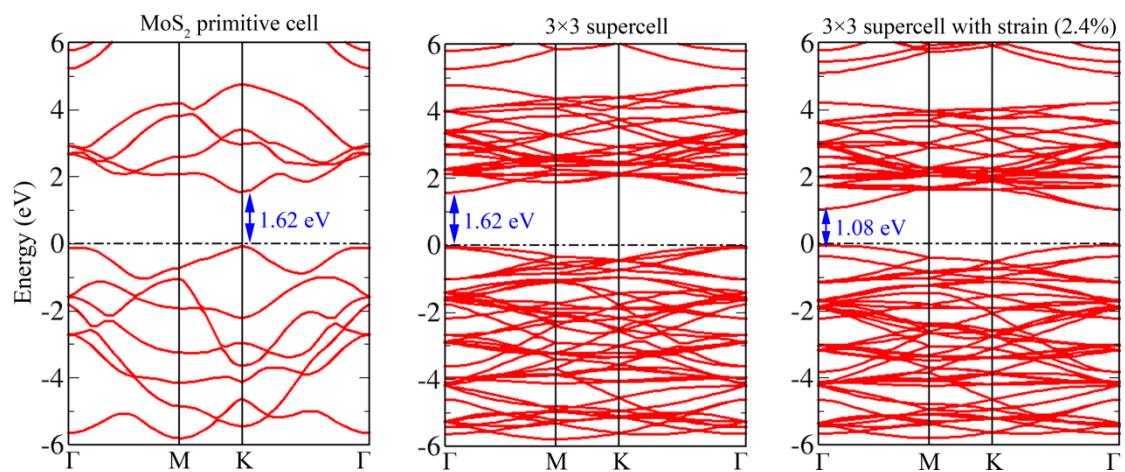


Figure S1 The band structure of 1×1 MoS₂ primitive cell (left), 3×3 MoS₂ supercell (middle), and 3×3 MoS₂ supercell with strain of 2.4% (right).

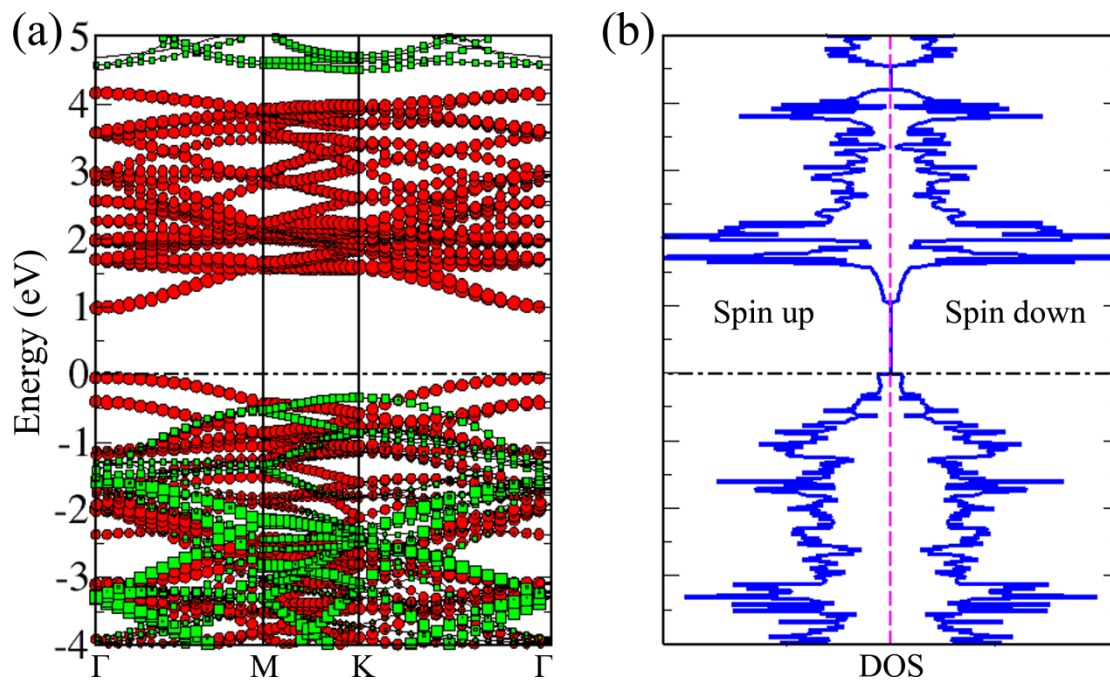


Figure S2 The spin-polarization (a) band structures and (b) DOS of hBN/MoS₂ bilayer heterostructures. The red circles and green squares respectively represent the projection to MoS₂ and hBN in hBN/MoS₂ bilayer heterostructures. The Fermi level is set to zero.

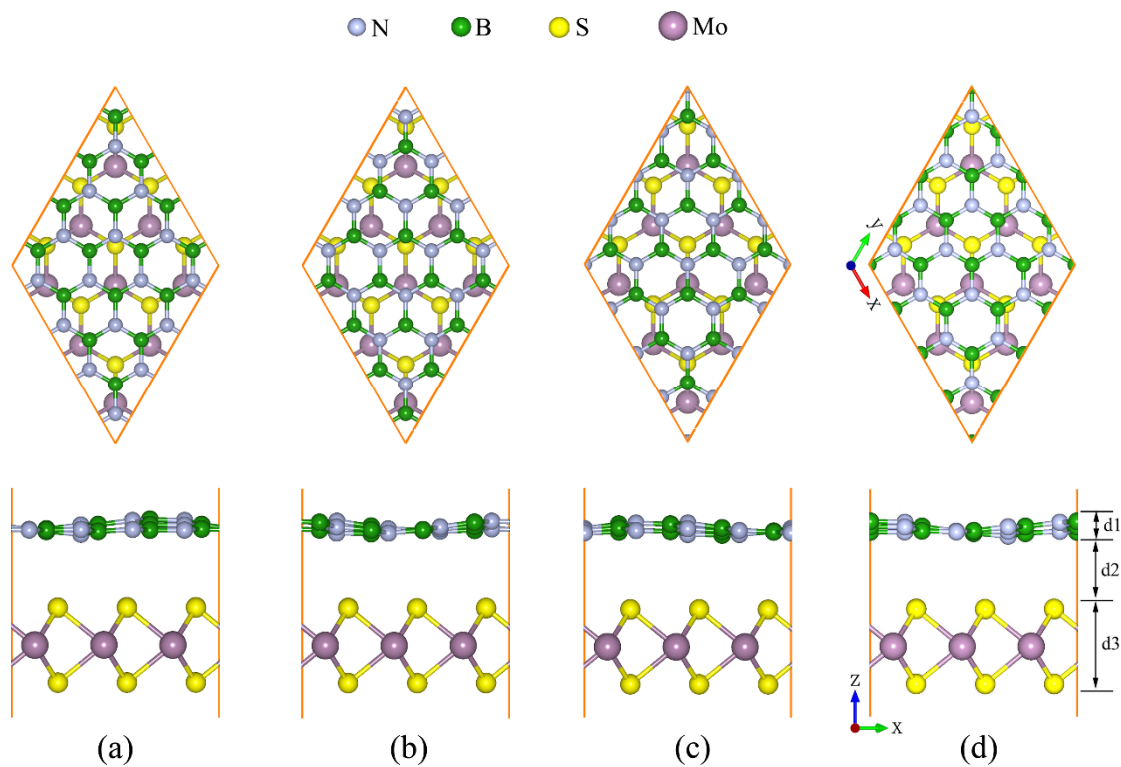


Figure S3 The top (up) and side (down) views of four different stacking patterns for hBN/MoS₂ bilayer heterostructures. The B, N, S, and Mo atoms are denoted by green, gray, yellow, and light magenta spheres, respectively. d_1 , d_2 , and d_3 stand for the buckling height of single-layer hBN, the interlayer spacing between the two layers, and the S-S vertical distance in MoS₂ monolayer, respectively.

Supplementary Table 1. The binding energy E_b between hBN flakes and MoS₂ monolayer. The buckling height d_1 , interlayer spacing d_2 , and the MoS₂ monolayer thickness d_3 for the four different stacking patterns of hBN/MoS₂ bilayer heterostructures, as well as the n-hBN/MoS₂ multilayer heterostructures, herein n denotes the layer number of hBN flakes.

system	configuration	E_b (eV)	d_1 (Å)	d_2 (Å)	d_3 (Å)
MoS ₂					3.119
hBN/MoS ₂	a	-1.511	0.603	2.996	3.067
	b	-1.498	0.508	3.037	3.070
	c	-1.497	0.486	3.044	3.078
	d	-1.514	0.604	2.983	3.065
n-hBN/MoS ₂	n=2	-4.110	0.387	3.058	3.068
	n=3	-6.885	0.338	3.060	3.068
	n=4	-9.398	0.287	3.068	3.068
	n=5	-12.137	0.286	3.087	3.069
	n=6	-14.910	0.285	3.110	3.069

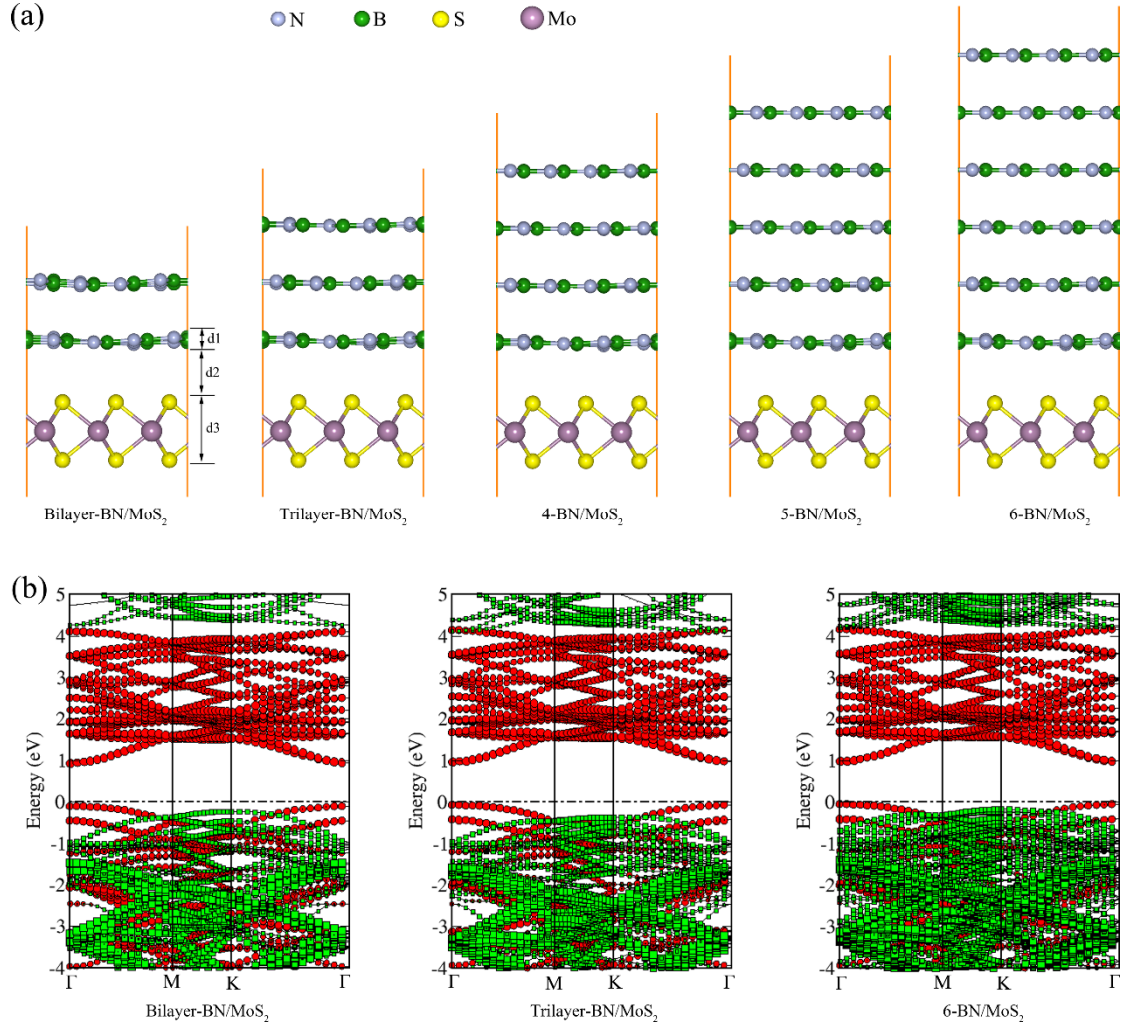


Figure S4 (a) The side views of n -hBN/MoS₂ multilayer heterostructures, $n=2,3,4,5,6$. (b) Projected band structures of bilayer-hBN/MoS₂, trilayer-hBN/MoS₂, and 6-hBN/MoS₂ multilayers without applying external E -field. The red circles and green squares respectively represent the projection to MoS₂ and hBN in these n -hBN/MoS₂ heterostructures. The Fermi level is set to zero.

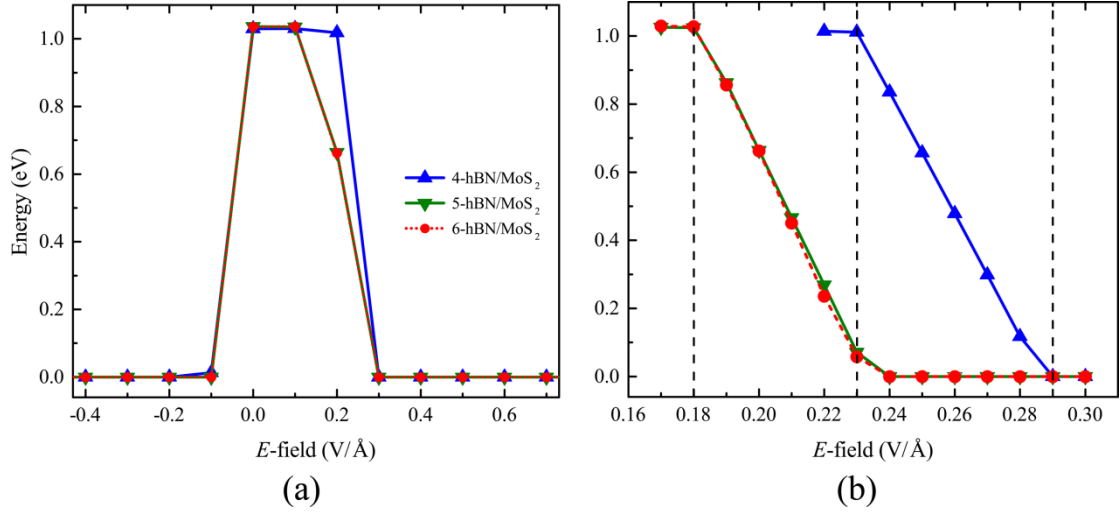


Figure S5 (a) A brief profile of energy gaps versus applied perpendicular E -field for 4-hBN/MoS₂, 5-hBN/MoS₂, and 6-hBN/MoS₂ heterostructures. (b) The detailed variations of energy gaps as a function of E -field for 4-hBN/MoS₂, 5-hBN/MoS₂, and 6-hBN/MoS₂ heterostructures corresponding to the E -field-tunable direct band gap range.

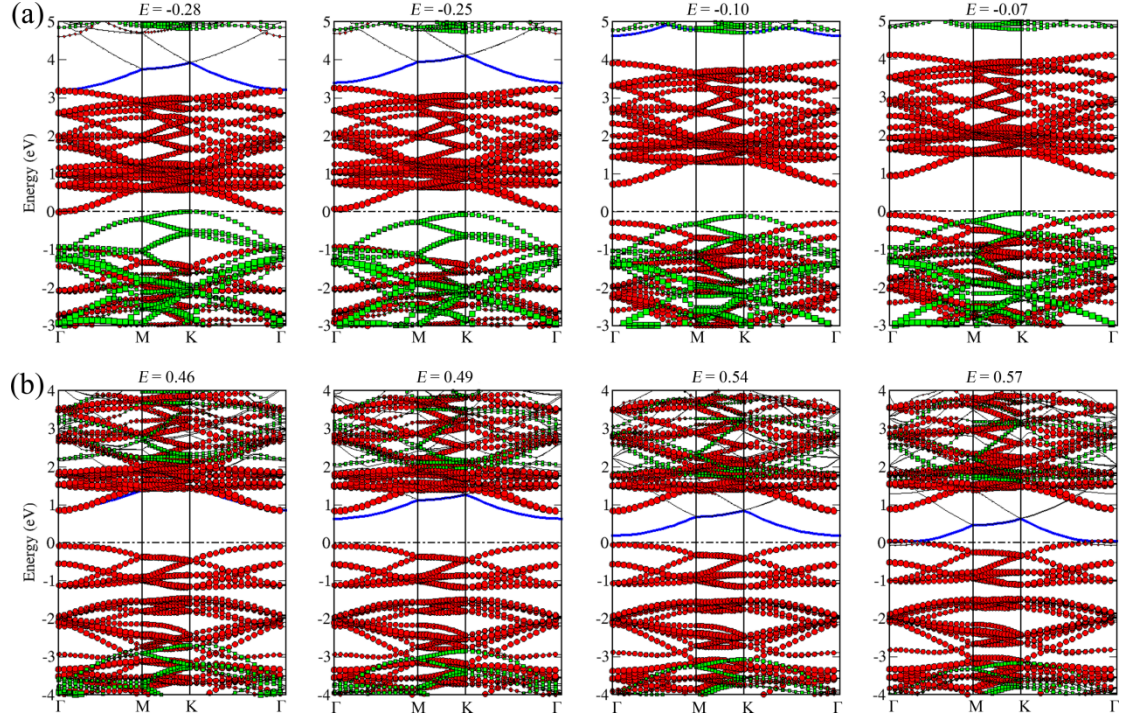


Figure S6 (a) Projected band structures of hBN/MoS₂ bilayer heterostructure in E -field-tunable indirect band gap range, under a backward vertical E -field of -0.28, -0.25, -0.10, and -0.07 V/Å. (b) Projected band structures of hBN/MoS₂ bilayer heterostructure in E -field-tunable direct band gap range, with a forward vertical E -field of 0.46, 0.49, 0.54, and 0.57 V/Å. The red circles and green squares respectively represent the projection to MoS₂ and hBN in the hBN/MoS₂ bilayer. The blue lines denote the γ -band. The Fermi level is set to zero.

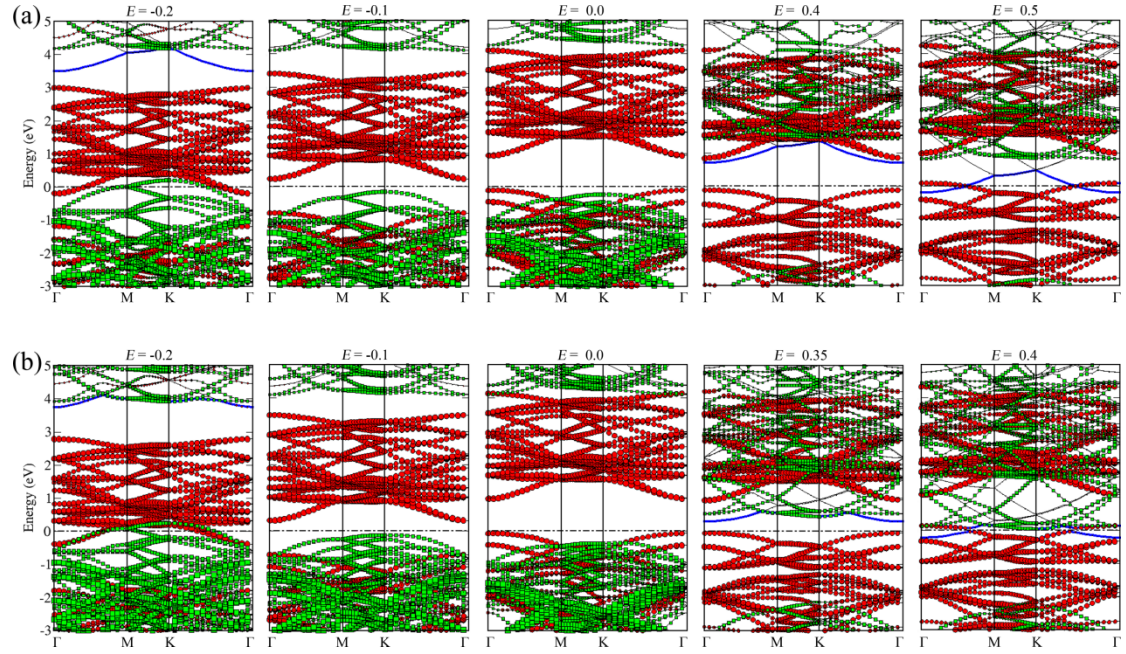


Figure S7 (a) Projected band structures of bilayer-hBN/MoS₂ heterostructure under a vertical E -field of -0.2, -0.1, 0, 0.4, and 0.5 V/Å. (b) Projected band structures of trilayer-hBN/MoS₂ heterostructure under a vertical E -field of -0.2, -0.1, 0, 0.35 and 0.4 V/Å. The red circles and green squares respectively represent the projection to MoS₂ and hBN in the hBN/MoS₂ bilayer. The blue lines denote the γ -band. The Fermi level is set to zero.